The Astrophysical Journal, 597:L173–L176, 2003 November 10

WHY SOLAR MAGNETIC FLUX CONCENTRATIONS ARE BRIGHT IN MOLECULAR BANDS

M. Schüssler,[1] S. Shelyag,[1] S. Berdyugina,[2] A. Vögler,[1] and S. K. Solanki[1]

Received 2003 August 19; accepted 2003 September 22; published 2003 October 17

ABSTRACT

Using realistic ab initio simulations of radiative magnetoconvection, we show that the bright structures in images taken in the "G band," a spectral band dominated by lines of the CH molecule, precisely outline small-scale concentrations of strong magnetic fields on the visible solar surface. The brightening is caused by a depletion of CH molecules in the hot and tenuous magnetic structures, thus confirming the model of radiatively heated magnetic flux concentrations. These results provide a firm basis for observational studies of the evolution and dynamics of the small-scale solar magnetic field derived through "proxy magnetometry" with G-band images.

Subject headings: Sun: magnetic fields — Sun: photosphere

On-line material: color figure

1. INTRODUCTION

Small-scale magnetic flux concentrations (magnetic elements) with field strengths of about 1500 G (150 mT) in the solar surface layers comprise a significant fraction of the magnetic flux (and almost all of the magnetic energy) in the solar atmosphere outside sunspots. The dynamical evolution, motion, and interaction of these concentrated elements of magnetic flux are crucial for the heating of the corona (Parker 1983; Schrijver et al. 1998) as well as for the total and spectral irradiance variations of the Sun (Spruit 2000; Fligge, Solanki, & Unruh 2000; Krivova et al. 2003). The difficulty of observing these small-scale (<100 km) flux concentrations through the turbulent atmosphere of the Earth has so far prevented a systematic investigation of their intrinsic spatial and temporal scales by direct measurements of the magnetic field through Zeeman polarimetry. Observers have therefore resorted to bright structures in the continuum light or in spectral lines considered to be "proxies" for magnetic flux concentrations. Images of the solar surface layers taken in Fraunhofer's G band, a spectral region around 430 nm, which is dominated by molecular lines near the CH band head, show conspicuous bright structures in the convective downflow regions (Muller & Roudier 1984; Muller 1985; Berger & Title 1996; Rutten et al. 2001; Langhans, Schmidt, & Tritschler 2002), where most of the concentrated magnetic flux is expected to reside (Weiss, Proctor, & Brownjohn 2002; Keller 1992; Domínguez Cerdeña, Kneer, & Sánchez Almeida 2003). Much of our current knowledge about the structure, distribution, and dynamics of small-scale magnetic features is based on G-band observations under the assumption that G-band bright points represent magnetic flux concentrations (Berger et al. 1995, 1998; van Ballegooijen et al. 1998; De Pontieu 2002). Such a correlation is supported observationally by the close association of bright structures in G-band filter images and magnetic flux concentrations measured in simultaneous magnetograms taken in moments of exceptionally good observing conditions (Berger & Title 2001). G-band movies are particularly useful for studying solar magnetic structure since they represent the only existing data in which both magnetic flux and convective motion are simultaneously imaged with high contrast; magnetograms show only the flux, while continuum movies show only the convection (sometimes with low-contrast magnetic features in the intergranular lanes).

Here we report a physical basis for such "proxy magnetometry" by unraveling the relationship between G-band brightness and magnetic flux using realistic ab initio three-dimensional simulations of radiative magnetoconvection in the solar surface layers. We find that the bright features in synthetic G-band spectra and filter images, calculated from the models, outline the magnetic flux concentrations, including fine details in their spatial patterns. The physical origin of the brightening is the high temperature and low density in the magnetic flux concentrations, which strongly reduces the concentration of CH molecules.

2. NUMERICAL SIMULATIONS AND SPECTRAL SYNTHESIS

So far, most theoretical attempts to study the relationship between G-band brightness and magnetic structure (Sánchez Almeida et al. 2001; Steiner, Hauschildt, & Bruls 2001; Kiselman, Rutten, & Plez 2001) have been based on ad hoc or semiempirical models of photospheric magnetic flux tubes. In contrast, our results are based on a self-consistent magnetic and atmospheric structure from a numerical three-dimensional compressible magnetohydrodynamic simulation including a realistic description of the radiative energy exchange in the solar photosphere (Vögler et al. 2003; Vögler & Schüssler 2003). The code used is based on a spatial and temporal fourth-order numerical scheme for the MHD equations and on a module for nongray radiative transfer with a short-characteristic integration along rays and opacity binning, which have been extensively tested (Vögler 2003).[3] Here we consider a simulation run corresponding to a small part of a magnetically active region on the Sun. The dimensions of the computational box are 1400 km in the vertical direction (covering the range between 800 km below and 600 km above the visible solar surface) and 6000 km in both horizontal directions, with grid spacings of 14 and 21 km, respectively. The side boundaries are periodic, while the lower boundary allows for free in- and outflow of matter. The box is penetrated by a fixed amount of vertical magnetic flux corresponding to an average vertical magnetic field strength (flux density) of 200 G (20 mT). We consider a snapshot taken about 160 (solar) minutes after the start of the simulation. At this time, a statistically stationary

[1] Max-Planck-Institut für Aeronomie, Max-Planck-Strasse 2, 37191 Katlenburg-Lindau, Germany; schuessler@linmpi.mpg.de, shelyag@linmpi.mpg.de, voegler@linmpi.mpg.de, solanki@linmpi.mpg.de.

[2] Institut für Astronomie, ETH Zürich, ETH-Zentrum CH-8092, Switzerland; sveta@astro.phys.ethz.ch.

[3] See http://www.linmpi.mpg.de/~msch/Thesis_Voegler.pdf.

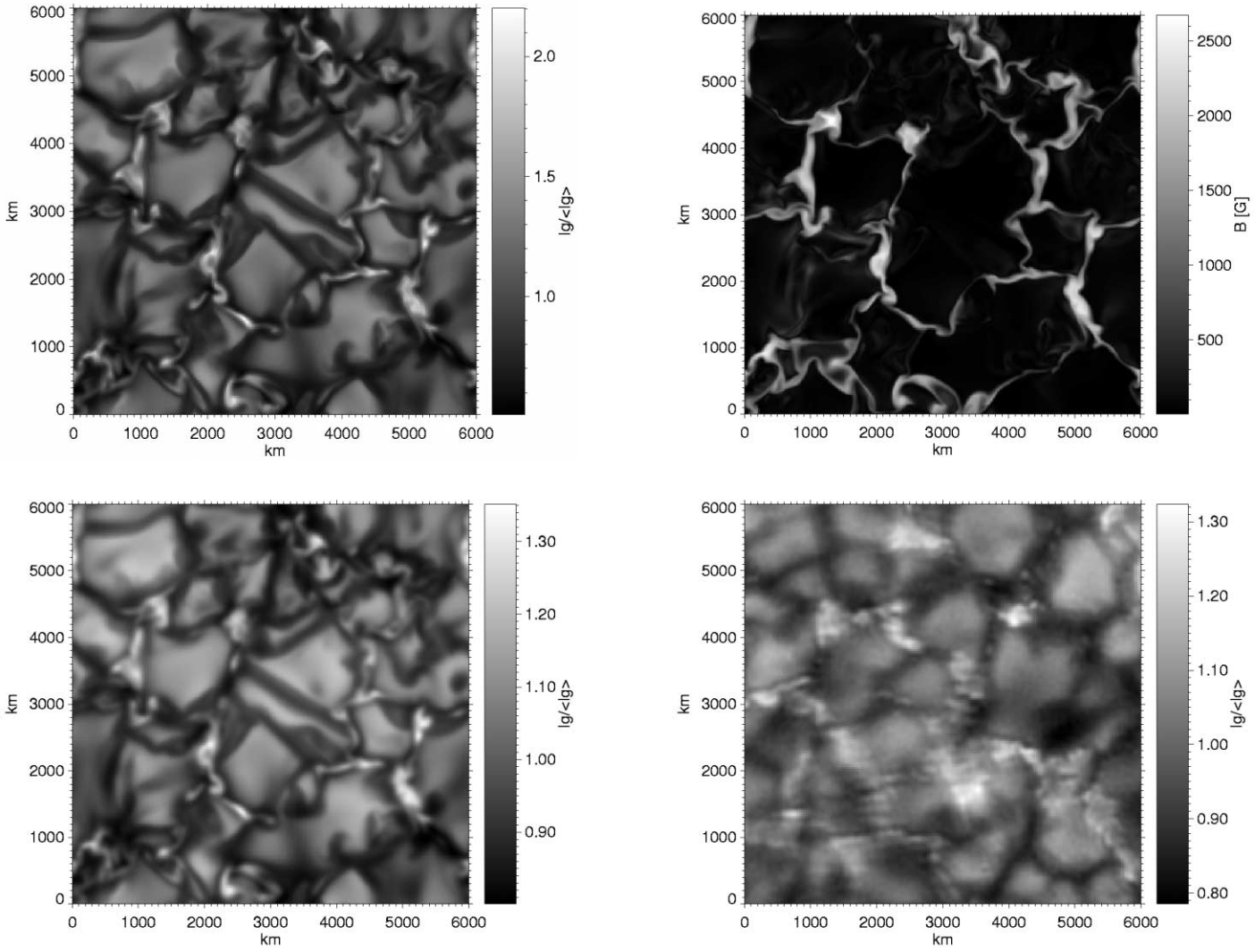

FIG. 1.—Simulated and observed images of the G-band contrast (local G-band brightness divided by spatial average: $I_g/\langle I_g \rangle$) and magnetic structure at the solar surface. *Upper left:* Synthetic filter image of the simulation area (6000 × 6000 km^2) in the G-band spectral region around 430 nm. The extended bright regions are convective upwellings (granules) surrounded by a network of dark downflow lanes. The small brilliant patches in the dark areas coincide with magnetic flux concentrations. *Upper right:* Gray shading of the magnetic field strength (in units of gauss) at the same time step as the G-band contrast image. About two-thirds of the vertical magnetic flux penetrating the simulation box has been assembled into flux concentrations with a field strength above 1000 G (100 mT). *Lower left:* G-band image after spatial smoothing mimicking the diffraction by a telescope of 1 m aperture and the image degradation by the Earth's atmosphere. *Lower right:* Observed G-band image of the same size as the simulated image with about the same area fraction of G-band bright points as in the simulation (subfield of an image that was taken with the SST on La Palma, courtesy of the Royal Swedish Academy of Sciences). [*See the electronic edition of the Journal for a color version of this figure.*]

state of the simulated radiative magnetoconvection has developed, in which the major part of the magnetic flux has been assembled in strong flux concentrations in the convective downflow regions (see Fig. 1, *upper right panel*).

Using the atmospheric structure from the simulation, we have first determined the concentration of CH molecules based on a chemical equilibrium of 270 molecular species and the 33 most abundant atoms (Berdyugina, Solanki, & Frutiger 2003), including all species that affect the CH equilibrium. We have then calculated the G-band spectrum emerging along vertical rays for each of the 288^2 horizontal grid cells of the simulation box under the assumption of local thermodynamic equilibrium. This seems to be well justified since (1) photodissociation of CH through bound levels of excited states is negligible in the solar atmosphere (Sánchez Almeida et al. 2001), (2) the ionization energy of carbon is high, and it remains primarily neutral in the solar atmosphere, so there are no effects due to overionization as they may occur for molecules with metal compounds, and (3) there is no scattering polarization observed in CH lines within the G band at the solar limb in quiet regions, indicating that the line formation is controlled by collisions rather than radiative processes (Gandorfer 2002).

Our synthetic G-band spectra have 2055 frequency points in the wavelength range between 429.5 and 431.5 nm and include 241 CH lines and 87 atomic lines (mainly from neutral iron). In order to obtain G-band images, the spectra are multiplied by a filter function mimicking the characteristics of filters used for observation (a central wavelength of 430.5 nm, and a FWHM of 1.2 nm) and integrated over wavelength.

Figure 1 shows a synthetic G-band image (*upper left panel*) together with a simultaneous map of the magnetic field strength (*upper right panel*) on the visible solar surface (the surface with

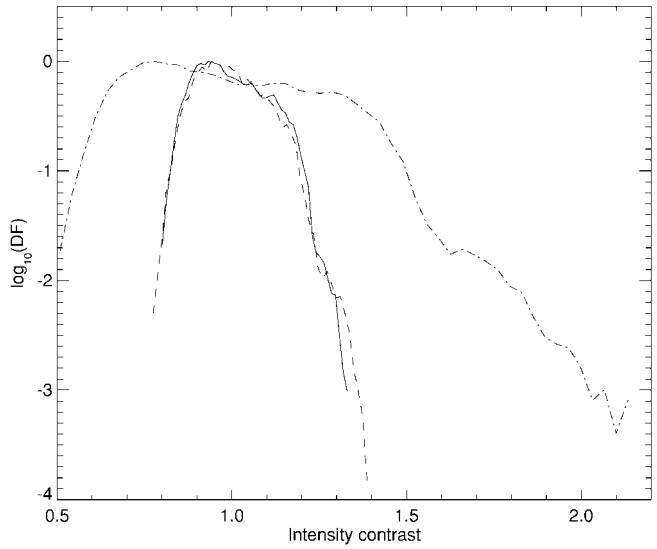

FIG. 2.—Normalized distribution function (DF) of the G-band contrast (local intensity divided by spatially averaged intensity) for the observed image (*dashed line*) and for the smoothed simulated image (*solid line*) after application of a combination of an Airy function (representing the finite telescope aperture) and a Lorentz function (describing the image degradation by turbulence in the Earth's atmosphere). The dotted line shows the DF of the unsmoothed simulated image, which shows that the actual G-band contrasts of the brightest points are expected to be significantly larger than the values given by the best ground-based observations available today. The only adjustable parameter for the description of the image degradation is the "damping coefficient," which determines the width of the Lorentz function.

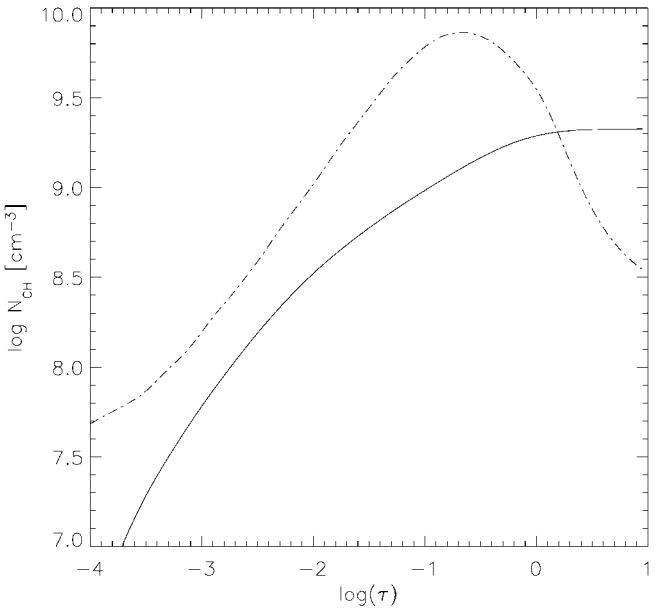

FIG. 3.—Number density of CH molecules, N_{CH}, as a function of continuum optical depth at 500 nm, τ. The dashed line corresponds to the average weakly magnetized ($B < 50$ G) atmosphere of the simulation snapshot shown in Fig. 1, and the solid line corresponds to the average atmosphere of the bright magnetic elements with a field strength above 1000 G and a G-band intensity above 1.5 of the average value. The CH lines in the G band are formed around $\log \tau = -1$. In this layer, the number density of CH is reduced by more than factor of 6 within the magnetic flux concentrations in comparison with the average atmosphere. This drop of the CH concentration is due to a 17% higher temperature (corresponding to about 900 K) and a 30% lower density within the magnetic flux concentration in the range of optical depth where the spectral lines of CH are formed. A low number density of CH leads to less absorption in the CH lines and thus larger G-band brightness.

a continuum optical depth of unity). There is a nearly perfect correspondence between the localized G-band brightenings in the network of dark convective downflow lanes (between the more extended bright upflows) and the patches of concentrated magnetic field; even fine details of the magnetic field pattern are reflected in the G-band intensity. About 98% of all points in the downflow regions with a G-band contrast of greater than 1.5 with respect to the average G-band brightness have a magnetic field strength exceeding 1000 G. The correlation coefficient between G-band brightness and magnetic field strength in the downflow regions is 0.73, which has an extremely high significance owing to the large number of points.

The lower part of Figure 1 shows a comparison between the spatially smoothed simulated G-band image (*lower left panel*) and a subfield of the same physical size from an observed G-band image taken with the Swedish Solar Telescope (SST) on La Palma (Canary Islands, Spain). The point-spread function used for smoothing of the simulated image is a combination of an Airy function corresponding to the 1 m aperture of the telescope and a Lorentz function describing the image degradation by turbulence in the terrestrial atmosphere (Nordlund 1984). The width of the Lorentz function has been determined by comparing the distribution functions of the G-band contrast for the observed and the smoothed simulated image. Figure 2 shows that such smoothing leads to a nearly perfect agreement of the distribution functions over the whole range of G-band brightness.

The qualitative similarity of the simulated and observed images in the lower part of Figure 1 is obvious: both images show bright, elongated features in the downflow regions and a disturbed convection pattern in regions with accumulations of bright features. There can be little doubt that the bright features in the observed image outline magnetic flux concentrations with kilogauss field strengths in the same way as in the simulation results. Note that the observed image has not been selected with regard to the best image quality but rather by requiring a similar area fraction of G-band bright points as in the simulation. It has also not undergone any image reconstruction procedure, which would lead to a better visual appearance but would affect the brightness distribution.

3. PHYSICAL ORIGIN OF THE G-BAND BRIGHTENING

Why are the G-band bright points so closely associated with the magnetic flux concentrations in the downflow regions? The enhanced G-band brightness of the granules is mostly due to their larger continuum intensity. While the magnetic elements also appear bright in the continuum radiation (Vögler & Schüssler 2003), their intensity contrast in the G band is much larger. This is due to the strong weakening of the absorption in the CH lines due to the depletion of CH molecules in the magnetic flux concentrations by the combined effects of a larger temperature (higher dissociation rate) and a lower density (less associative collisions). This is demonstrated in Figure 3, which shows the number density of CH molecules in the average weakly magnetized ($B < 50$ G) part of the atmosphere corresponding to the simulation snapshot given in Figure 1 in comparison with the average atmosphere of magnetic bright points (with a magnetic field strength above 1000 G and a G-band intensity larger than 1.5 times the average). The much lower CH concentration at the formation height of the CH spectrum

around log $\tau = -1$ leads to less absorption in the spectral lines of this molecule and thus, together with the higher level of continuum intensity, to a strongly increased brightness in the G band. The physical association of a large field strength with a higher temperature and a lower density can easily be understood in terms of lateral heating by radiation of the transparent tenuous interior of a flux concentration in lateral balance of the total (gas plus magnetic) pressure (Spruit 1976; Deinzer et al. 1984; Knölker et al. 1991; Vögler & Schüssler 2003). In fact, the strong flux concentrations in the simulations are found to be almost in total pressure equilibrium, showing values of the plasma beta (gas pressure divided by magnetic pressure) of the order of 0.1 around the average level of optical depth unity in the weakly magnetic part of the photosphere.

4. CONCLUSIONS

We have provided a quantitative reproduction of the observed G-band contrasts and their association with small-scale magnetic flux concentrations. Previous attempts to calculate G-band intensities have either relied on ad hoc and semiempirical models of the magnetic structure or resulted in too small G-band contrasts (Uitenbroek 2003). Our results are based on realistic radiative MHD simulations with high horizontal grid resolution (21 km) together with a very detailed treatment of the G-band spectrum synthesis. The excellent agreement between the output of our ab initio simulations and the very sensitive G-band brightness distribution confirms the physical model of magnetic flux concentrations as evacuated and laterally heated structures. Unraveling of the physical mechanism for the connection between G-band bright points and magnetic flux concentrations in the solar photosphere provides a firm basis for the observational study of small-scale magnetic field dynamics using G-band image series, which is important for understanding the physics behind solar irradiance variations and the magnetic heating processes of the solar chromosphere and corona.

This work has been supported by the Deutsche Forschungsgemeinschaft under grant Schu 500-7 in the framework of the priority research program SPP1035. The Max-Planck Institute for Aeronomy and University of Chicago Radiative Magnetohydrodynamics (MURAM) code, on which this work is based, has been developed in cooperation with F. Cattaneo, Th. Emonet, and T. Linde from the University of Chicago. The data from the SST on La Palma have been kindly provided by the Institute for Solar Physics of the Royal Swedish Academy of Sciences, Stockholm.

REFERENCES

Berdyugina, S., Solanki, S. K., & Frutiger, C. 2003, A&A, in press
Berger, T. E., Loefdahl, M. G., Shine, R. S., & Title, A. M. 1998, ApJ, 495, 973
Berger, T. E., Schrijver, C. J., Shine, R. A., Tarbell, T. D., Title, A. M., & Scharmer, G. 1995, ApJ, 454, 531
Berger, T. E., & Title, A. M. 1996, ApJ, 463, 365
———. 2001, ApJ, 553, 449
Deinzer, W., Hensler, G., Schüssler, M., & Weisshaar, E. 1984, A&A, 139, 426
De Pontieu, B. 2002, ApJ, 569, 474
Domínguez Cerdeña, I., Kneer, F., & Sánchez Almeida, J. 2003, ApJ, 582, L55
Fligge, M., Solanki, S. K., & Unruh, Y. C. 2000, A&A, 353, 380
Gandorfer, A. 2002, The Second Solar Spectrum, Vol. 2: 3910 Å to 4630 Å (Zürich: Hochsch. ETH Zürich)
Keller, C. U. 1992, Nature, 359, 307
Kiselman, D., Rutten, R. J., & Plez, B. 2001, in ASP Conf. Ser. 200, Recent Insights into the Physics of the Sun and Heliosphere, ed. P. Brekke, B. Fleck, & J. B. Gurman (San Francisco: ASP), 287
Knölker, M., Grossmann-Doerth, U., Schüssler, M., & Weisshaar, E. 1991, Adv. Space Res., 11(5), 285
Krivova, N. A., Solanki, S. K., Fligge, M., & Unruh, Y. C. 2003, A&A, 399, L1
Langhans, K., Schmidt, W., & Tritschler, A. 2002, A&A, 394, 1069
Muller, R. 1985, Sol. Phys., 100, 237
Muller, R., & Roudier, Th. 1984, Sol. Phys., 94, 33
Nordlund, Å. 1984, in Small-Scale Dynamical Processes in Quiet Stellar Atmospheres, ed. S. L. Keil (Sunspot: Sacramento Peak Obs.), 174
Parker, E. N. 1983, ApJ, 264, 635
Rutten, R. J., Hammerschlag, R. H., Sütterlin, P., & Bettonvil, F. C. M. 2001, in ASP Conf. Ser. 236, Advanced Solar Polarimetry—Theory, Observation, and Instrumentation, ed. M. Sigwarth (San Francisco: ASP), 25
Sánchez Almeida, J., Asensio Ramos, A., Trujillo Bueno, J., & Cernicharo, J. 2001, ApJ, 555, 978
Schrijver, C. J., et al. 1998, Nature, 394, 152
Spruit, H. C. 1976, Sol. Phys., 50, 269
———. 2000, Space Sci. Rev., 94, 113
Steiner, O., Hauschildt, P. H., & Bruls, J. 2001, A&A, 372, L13
Uitenbroek, H. 2003, in ASP Conf. Ser. 286, Current Theoretical Models and Future High Resolution Solar Observations: Preparing for ATST, ed. A. A. Pevtsov & H. Uitenbroek (San Francisco: ASP), 403
van Ballegooijen, A. A., Nisenson, P., Noyes, R. W., Löfdahl, M. G., Stein, R. F., Nordlund, Å., & Krishnakumar, V. 1998, ApJ, 509, 435
Vögler, A. 2003, Ph.D. thesis, Univ. Göttingen
Vögler, A., & Schüssler, M. 2003, Astron. Nachr., 324, 399
Vögler, A., Shelyag, S., Schüssler, M., Cattaneo, F., Emonet, T., & Linde, T. 2003, in Modelling of Stellar Atmospheres, ed. N. E. Piskunov, W. W. Weiss, & D. F. Gray (San Francisco: ASP), in press
Weiss, N. O., Proctor, M. R. E., & Brownjohn, D. P. 2002, MNRAS, 337, 293